

See discussions, stats, and author profiles for this publication at: <https://www.researchgate.net/publication/7308105>

Crab Shell Chitin Whisker Reinforced Natural Rubber Nanocomposites. 1. Processing and Swelling Behavior

ARTICLE *in* BIOMACROMOLECULES · MAY 2003

Impact Factor: 5.75 · DOI: 10.1021/bm020127b · Source: PubMed

CITATIONS

202

READS

66

2 AUTHORS:



G. Kalaprasad

University of Calicut

13 PUBLICATIONS 1,067 CITATIONS

SEE PROFILE



Alain Dufresne

Grenoble Institute of Technology

313 PUBLICATIONS 15,353 CITATIONS

SEE PROFILE

Crab Shell Chitin Whisker Reinforced Natural Rubber Nanocomposites. 1. Processing and Swelling Behavior

Kalaprasad Gopalan Nair and Alain Dufresne*

Centre de Recherches sur les Macromolécules Végétales (CERMAV-CNRS), Université Joseph Fourier,
BP 53, F 38041 Grenoble Cedex 9, France

Received November 13, 2002; Revised Manuscript Received January 22, 2003

Nanocomposite materials were obtained from a colloidal suspension of chitin whiskers as the reinforcing phase and latex of both unvulcanized and prevulcanized natural rubber as the matrix. The chitin whiskers, prepared by acid hydrolysis of chitin from crab shell, consisted of slender parallelepiped rods with an aspect ratio close to 16. After the two aqueous suspensions were mixed and stirred, solid composite films were obtained either by freeze-drying and hot-pressing or by casting and evaporating the preparations. The processing and swelling behavior of composite films were evaluated. It was concluded that the whiskers form a rigid network assumed to be governed by a percolation mechanism in the evaporated samples only. Comparatively, better resistance of evaporated samples than hot-pressed ones against swelling in an organic solvent medium is good evidence for the existence of a rigid chitin network. The values of diffusion coefficient, bound rubber content, and relative weight loss also supported the presence of a three-dimensional chitin network within the evaporated samples. The mechanical behavior of the composites gives additional insight and evidence for this fact (part 2).

Introduction

Latex from rubber trees (*Hevea brasiliensis*) is virtually the source of all commercial natural rubber (NR) (*cis*-1,4-polyisoprene). Both NR and its synthetic counterpart, styrene butadiene rubber (SBR) display mechanical properties which make them important and irreplaceable materials in dynamically loaded applications such as tires and engine mounts.¹ NR is mainly used in winter tires and in tires for trucks. Small solid tires are usually made of SBR. The consumption of NR and SBR is equal, and the materials can be used interchangeably. The unique mechanical properties of NR result from both its highly stereoregular microstructure and the rotational freedom of the α -methylenic C—C bonds and from the entanglements resulting from the high molecular weight which contributes to its high elasticity.

The properties of NR can be tailored by the addition of fillers of varying surface chemistry and aggregate size/aspect ratio to suit the application concerned. Carbon black and silica are the main fillers used in the compounding recipes.^{2,3} Short fibers can be used to reinforce polymers in order to improve or modify certain mechanical properties of the host matrix for specific applications.⁴ The reinforcement of rubber with fibers combines the elastic behavior of the rubber with the strength and stiffness of the reinforcing phase.^{5–7} The use of various natural fibers such as bamboo, coir, and oil palm as reinforcing agents in rubber matrixes has been reported.^{8–13}

Nanocomposites are relatively a new class of composites that exhibit ultrafine phase dimensions of 1–1000 nm.

Because of the nanometric size effect, these composites have some unique outstanding properties with respect to their conventional microcomposite counterparts. As most of the present-day polymers used for preparing nanocomposites are synthetic materials, their processability, biocompatibility, and biodegradability are much more limited than those of natural polymers. Compared to the studies in the field of conventional microcomposites and nanocomposites based on synthetic non-biodegradable materials, only limited work has been reported in the area of bionanocomposites, especially chitin-based nanocomposites. Another advantage of the natural nanofillers is their availability and their resulting lower cost relative to synthetic nanofillers.

Chitin constitutes the structure of the external skeleton in shellfish and insects and is one of the major components of the fibrous material of cellular walls in mushrooms and algae.^{14,15} It is estimated that about 10^{10} to 10^{11} tons of this polymer are synthesized each year. Zooplankton cuticles (in particular small shrimps constituting krill) are the most important source of chitin. However, fishing of these tiny organisms (a few millimeters in length) is too difficult to consider for any industrial use. Shellfish canning industry waste (shrimp or crab shells) in which the chitin content ranges between 8 and 33% constitutes the main source of this polymer. Native chitin is highly crystalline and depending on its origin it occurs in three forms identified as α -, β -, and γ -chitin. In the former, all chains are arranged in an antiparallel fashion with strong intermolecular hydrogen bonding. It is the dominant and stable form since it constitutes arthropod cuticles and mushroom cellular walls. Chitin has been known to form microfibrillar arrangements embedded in a protein matrix, and these microfibrils have

* To whom correspondence should be addressed (e-mail: Alain.Dufresne@cermav.cnrs.fr).

diameters ranging from 2.5 to 2.8 nm.¹⁶ Crustacean cuticles possess chitin microfibrils with diameters as large as 25 nm.^{17,18}

By analogy with previous works performed in our laboratory and which deal with cellulose or starch microcrystal reinforced nanocomposite systems,^{19–28} chitin whiskers were used as a reinforcing phase in a polymeric matrix. Suspensions of chitin crystallites were prepared as described by Revol and Marchessault^{29–32} by acid hydrolysis of chitin obtained from crab shells. The object of this treatment was to dissolve away regions of low lateral order so that the water-insoluble, highly crystalline residue may be converted into a stable suspensoid by subsequent vigorous mechanical shearing action. Preliminary studies were performed with chitin whiskers obtained from squid pen³³ and *Riftia* tubes³⁴ as the reinforcing phase and a copolymer of styrene and butyl acrylate³³ or poly(caprolactone)³⁴ as the matrix.

In this study chitin whiskers were obtained from crab shells. The limb of crab (red crab) used in this study is the main source for the production of chitin because it is relatively rich in chitin. The preparation of the suspensions of chitin whiskers is described, and the resulting nanocrystalline chitin fragments are characterized. Nanocomposite materials were processed using either unvulcanized or vulcanized NR as the host matrix. For unvulcanized NR latex based nanocomposites, two processing techniques, viz., water evaporation and freeze-drying followed by a hot-pressing step, were used to investigate the effect of the processing method on the material properties. The morphology and swelling behavior in an organic medium of composite films were investigated.

Experimental Section

Chitin Whiskers. The raw original material consists of chitin from crab shells obtained from Aldrich (ref 41,795-5). Suspensions of chitin whiskers were prepared from this material based on the method described elsewhere for squid pen³³ and *Riftia* tubes.³⁴ It was adapted to account for the source of chitin. Samples were first boiled and stirred in a 5% KOH solution for 6 h to remove most of the proteins. This suspension was subsequently kept at room temperature overnight under stirring, filtered, and washed several times with distilled water. Chitin samples were then bleached with 17 g of NaClO₂ in 1 L of water containing 0.3 M sodium acetate buffer, for 6 h at 80 °C. The bleaching solution was changed every 2 h followed by abundant rinsing the sample with distilled water. After the samples were bleached, the suspension was kept in a 5% KOH solution for 48 h to remove residual proteins. The resulting suspension was centrifuged at 3600 rpm for 15 min.

Protein-free chitin whiskers suspension was prepared by hydrolyzing the purified chitin sample with 3 N HCl at the boil for 90 min under stirring. The ratio of 3 N HCl to chitin was 30 cm³·g⁻¹. After acid hydrolysis, the suspension was diluted with distilled water followed by centrifugation (36000 rpm for 15 min). This process was repeated three times. Next, the suspension was transferred to a dialysis bag and dialyzed in running water for 2 h and then overnight in distilled water

Table 1. Codification of the Samples

sample	processing technique	matrix	chitin content (wt %)	chitin content (vol %)
NRev	water evaporation	unvulc.NR	0	0
NCH2ev		unvulc.NR	2	1.34
NCH5ev		unvulc.NR	5	3.39
NCH10ev		unvulc.NR	10	6.90
NCH15ev		unvulc.NR	15	10.5
NCH20ev		unvulc.NR	20	14.3
PNRev	water evaporation	prevulc.NR	0	0
PCH2ev		prevulc.NR	2	1.34
PCH5ev		prevulc.NR	5	3.39
PCH10ev		prevulc.NR	10	6.90
PCH15ev		prevulc.NR	15	10.5
PCH20ev		prevulc.NR	20	14.3
NRL	freeze-drying and hot-pressing	unvulc.NR	0	0
NCH5L		unvulc.NR	5	3.39
NCH10L		unvulc.NR	10	6.90
NCH15L		unvulc.NR	15	10.5
NCH20L		unvulc.NR	20	14.3

until a pH = 4 was reached. The dispersion of whiskers was completed by a further 5-min ultrasonic treatment for every 30-cm³ aliquot. It was subsequently stored at 6 °C after adding sodium azoture to avoid bacterial growth until used.

Natural Rubber. Natural rubber (NR) was kindly supplied as unvulcanized NR latex by the Technical Center, MAPA, Liancourt, France. It contained spherical particles with an average diameter around 1 μm and had a TSC (total solid content) and a DRC (dry rubber content) of 61.58% and 60.1%, respectively. Sodium lauryl sulfate (0.2 g/100 g of dry rubber) and potassium (0.4 g/100 g of dry rubber) were added as stabilizers. The density of dry NR was 1 g·cm⁻³.

Prevulcanized latex with low degree of cross-linking was kindly provided by SAFIC ALCAN, Puteaux, France. Its TSC, DRC, and density were 61.5%, 60%, and 1 g·cm⁻³, respectively. Vulcanizing agents such as tetramethylthiuram disulfide (TMTD) and zinc oxide (ZnO) were used as accelerator and activator, respectively, in this latex. The latex particle size was around 1 μm.

Nanocomposites Processing. The suspension of whiskers and NR latex were mixed in various proportions in order to obtain final dry composite films ranging between 0.5 and 1 mm in thickness and with 0–20% weight fractions of solid chitin whiskers in NR matrix. Both unvulcanized and prevulcanized lattices were used in this study. After the samples were stirred, the preparations were cast in a Teflon mold and evaporated at 40 °C for 10–15 days (according to the water present in the medium) and after that at 80 °C for 1 h. For prevulcanized NR latex-based nanocomposites, the latter heat treatment (at 80°C) may improve film homogeneity and complete the chemical cross-linking process. Freeze-drying and subsequent and hot-pressed method was used only in the case of unvulcanized latex to make the composites. Hot-pressing was performed with a Carver laboratory press at 138 bar for 2 min at 100 °C.

The chitin volume content was calculated by taking 1.5 g·cm⁻³ for the density of crystalline chitin. Sample details and their abbreviations used in this study are listed in Table 1.

Microscopies. Transmission electron microscopy (TEM) observations were made with a Philips CM200 electron microscope. A droplet of a dilute suspension of chitin whiskers was deposited and allowed to dry on a carbon-coated grid. The accelerating voltage was 80 kV.

Scanning electron microscopy (SEM) was performed to investigate the morphology of the nanocomposite films with a JEOL JSM-6100 instrument. The specimens were frozen under liquid nitrogen, then fractured, mounted, coated with gold/palladium on a JEOL JFC-1100E ion sputter coater, and observed. SEM micrographs were obtained using 7 kV secondary electrons.

Infrared Spectroscopy. Measurements were performed with a Fourier transform infrared (FT-IR) spectrometer (Perkin-Elmer 1720 X).

Swelling Experiments. The kinetics of toluene absorption was determined for vulcanized NR based composites. The specimens used were thin disks with diameter of 7.5 mm and around 0.5–1 mm thick. The thickness, $2L$, of the film was therefore supposed to be thin enough so that the molecular diffusion was considered to be one-dimensional. After weighing, the samples were immersed in toluene. The samples were removed at specific intervals (t) and weighed (M_t) up to an equilibrium value (M_∞). The swelling rate of the samples was calculated by dividing the gain in weight ($M_t - M_0$) by the initial weight (M_0). The diffusion coefficient was determined from the initial slope of the plot of $(M_t - M_0)/M_\infty$ as a function of $(t/L^2)^{1/2}$. Details of the calculation can be found elsewhere.²⁶

These swelling experiments were more difficult to perform for unvulcanized materials since part of the sample could dissolve in toluene. Therefore the following analysis was performed for these samples. Thin disks of sample material were first weighed (M_0) and then immersed in toluene for 48 h. They were subsequently dried for 12 h at 55–60 °C and weighed again (M_0'). The “sol” fraction (M_0'/M_0) and relative weight loss ($\text{RWL} = [M_0 - M_0']/M_0$) were then determined. This allowed estimating the fraction of NR bonded to the filler and the fraction of NR dissolved in toluene.

Results and Discussions

Chitin Whiskers. Figure 1a shows a scanning electron micrograph of the raw original material consisting of commercial chitin from crab shells. It consists of a mixture of roughly spherical particles with diameter around 0.5–1 mm (partially shown on the right side in Figure 1a) and ill-defined particles. In the latter, the fibrillar arrangement of chitin is clearly evidenced. These particles are made up of intertwined chitin microfibrils.

After acid hydrolysis and under low stirring, the suspension of chitin microcrystals displays a colloidal behavior when observed in polarized light between crossed polars (Figure 1b). It is ascribed to the formation of birefringent domains. This colloidal behavior was previously observed for cellulose microcrystal suspensions.²¹ In the case of chitin, this is due to the presence of positive charges (NH_3^+) at the surface of the whiskers, resulting from the protonation of amino groups.²⁹

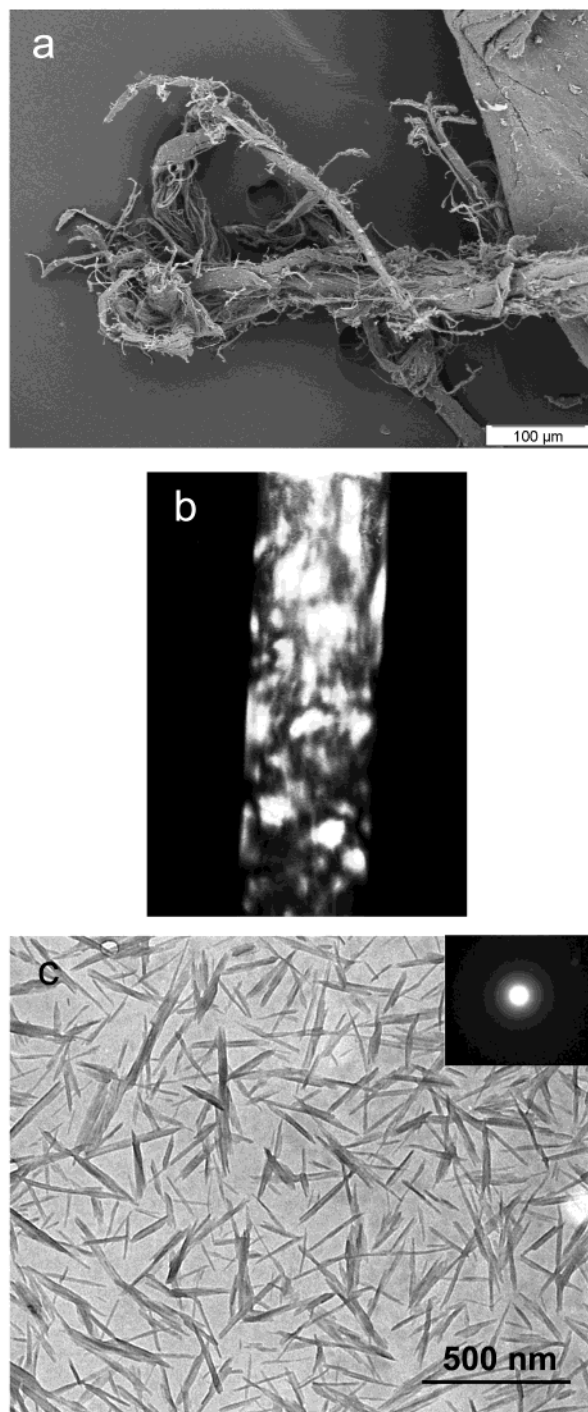


Figure 1. (a) Scanning electron micrograph of commercial chitin from crab shells. (b) Photograph of the suspension of chitin whiskers observed between cross nicols, showing the formation of birefringent domains. (c) Transmission electron micrograph of a dilute suspension of chitin whiskers (inset: typical electron diffractogram recorded on chitin fragments).

Figure 1c shows a transmission electron micrograph of a dilute suspension of hydrolyzed crab shell chitin. The suspension contains chitin fragments consisting of both individual microcrystals and associated or collapsed microcrystals. These chitin fragments consist of slender rods with sharp points that have a broad distribution in size. The dimensions of the whiskers were averaged on 111 representative items. The length distribution of these fragments has a typical histogram shown in Figure 2. They have a length

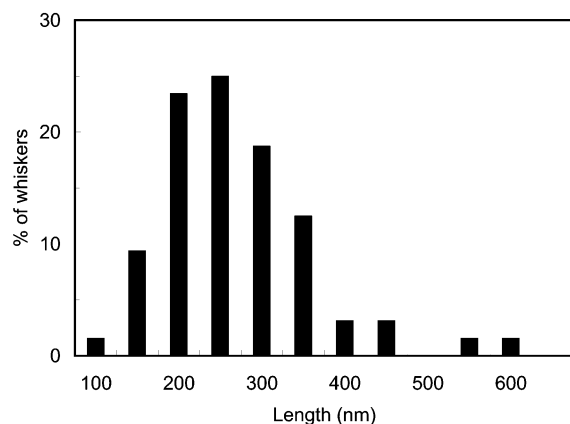


Figure 2. Histogram showing the length distribution of chitin whiskers extracted from crab shells obtained by hydrolysis with a hydrochloric acid solution.

ranging from 100 nm up to 600 nm and a width ranging from 4 to 40 nm. The exact determination of the latter was difficult because of both the tapering of the chitin fragments and the presence of narrow microcrystals. More than 75% of the whiskers have a length below 300 nm. The average length and width were estimated to be around 240 and 15 nm, respectively. The average aspect ratio (L/d , L being the length and d the diameter) of these whiskers is therefore around 16. These dimensions are close to those reported for chitin whiskers obtained from squid pen ($L = 50\text{--}300$ nm, $d = 10$ nm, $L/d = 15$)³³ but much lower than those observed for chitin whiskers obtained from *Riftia* tubes ($L = 0.5\text{--}10$ μm , $d = 18$ nm, $L/d = 120$).³⁴ The diffraction pattern obtained for chitin whisker suspension using transmission microscopy studies is also depicted in Figure 1c. Sharp and well-defined diffraction rings obtained indicate the crystalline nature (amorphous protein part and amorphous chitin domains have been removed during acid hydrolysis) of chitin whiskers present in the suspension.

For composite materials filled with crab shell chitin whiskers, interfacial phenomena are expected to be important owing to the high specific area of the filler ($\approx 180\text{ m}^2\cdot\text{g}^{-1}$). For example, for a 20 wt % chitin whisker filled composite, there are around 40 m^2 of filler surfaces in 1 cm^3 of the material.

An infrared spectrum was taken for a film of chitin whiskers obtained from the evaporation of the whisker suspension in order to display the absence of residual proteins on the chitin fragments (Figure 3). In the carbonyl region, the spectrum presents three strong absorption peaks at 1658, 1622, and 1556 cm^{-1} characteristic of anhydrous α -chitin.³⁵ The absence of the peak at 1540 cm^{-1} corresponding to the proteins³⁶ proves that the successive treatments were strong enough to eliminate all the proteins and to obtain pure chitin.

Morphology of Nanocomposites. An examination of the cryo fractured surface of chitin whisker/NR composites was carried out using SEM. Panels a and b of Figure 4 show the SEM of unfilled NRev and NRL films, respectively. The surface of unvulcanized NR latex evaporated film (NRev, Figure 4a) demonstrates a uniform phase morphology whereas freeze-dried and subsequent hot-pressed latex (NRL, Figure 4b) shows a nonuniform phase morphology. During the freeze-drying step, rubber chains present in the latex do

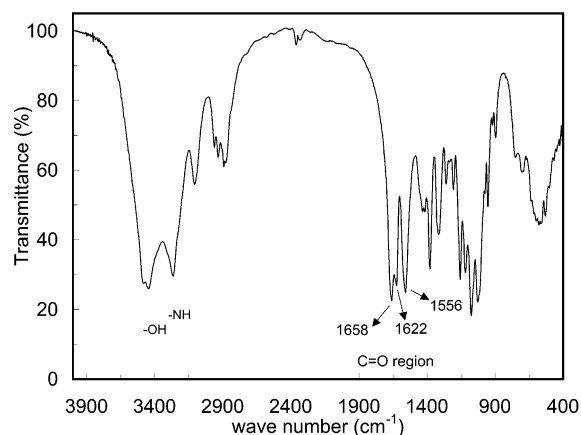


Figure 3. Fourier transform infrared spectrum taken for a film of chitin whiskers obtained from the evaporation of the whisker suspension.

not get enough time to orient themselves (interdiffusion) in a uniform manner because of the quenching prior to freeze-drying. As a result of this the molecular weight distribution becomes nonuniform, thus causing a nonuniform phase morphology on the surface as shown in Figure 4b. Another reason for the nonuniformity of the lyophilized film is the imperfection introduced by the evaporation of traces of entrapped water present in the freeze-dried rubber during hot-pressing. The surface of prevulcanized NR evaporated film (PNRev, Figure 4c) is found to be not so uniform as that of NRev as it constitutes certain spherical granular domains. This may be due to the retention of some original particulate structure formed as a result of the faster cross-linking nature of the surface molecules of the individual particles present in the prevulcanized latex.^{37,38}

Panels d–f of Figure 4 show the fractured surfaces of the composites filled with 20 wt % of chitin whiskers: NCH20ev, NCH20L, and PCH20ev, respectively. In Figure 4d, the chitin whiskers appear as white dots, which are distributed evenly throughout the unvulcanized evaporated matrix. The concentration of these white dots on the fractured surface of the composite was increased with increase in filler loading (not shown). A uniform distribution of whiskers in the matrix was clearly evidenced for all the compositions. The effect of the processing technique on the whisker distribution within the unvulcanized matrix can be studied by comparing panels d (evaporated film) and e (freeze-dried and hot-pressed film) of Figure 4. No clear difference can be reported. However, it seems that broader smooth unfilled regions are observed in Figure 4e. This could be an indication of poorer whisker distribution in freeze-dried and hot-pressed composites. The nonuniformity observed in Figure 4b seems to be absent for the composite (Figure 4e). This phenomenon is most probably the result of the increase in material stiffness upon the whisker addition. Panels d and f of Figure 4 reveal the effect of matrix cross-linking on the surface morphology of the composite. The comparison is difficult since the whiskers are not clearly evidenced in Figure 4f. However, the granular nature of the surface of prevulcanized NR-based composite is reported again. The cross-linked rubber molecules present in the latex prevent the uniform entrapment and distribution of whiskers in the matrix, thus making impenetrable domains to whiskers during film formation.

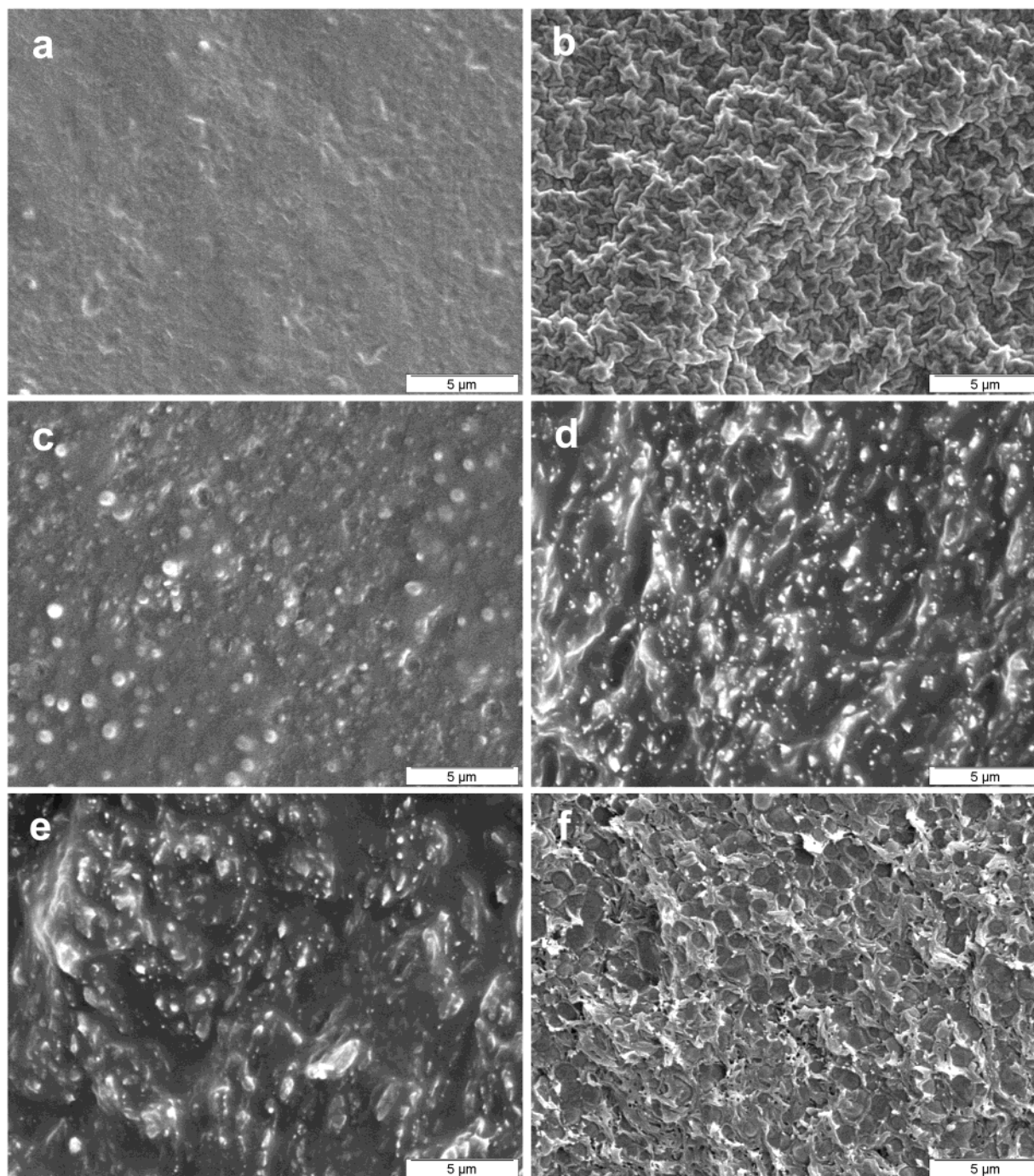


Figure 4. Scanning electron micrographs of the cryo-fractured surfaces of (a) Nrev, (b) NRL, (c) PNRev, (d) NCH20ev, (e) NCH20L, and (f) PCH20ev films.

Swelling Experiments. The swelling process and its kinetics give an idea about the capacity of a cross-linked polymer in different liquids and vapor media. The interaction of polymeric materials with solvents is a problem from both academic and technological points of view.³⁹ The mass and dimensions of polymer systems may be changed due to the penetration of solvents into swollen specimens. When a cross-linked polymer is brought into contact with a solvent, the network absorbs a certain amount of solvent, which depends strongly on the temperature, molecular weight of this solvent, the cross-linking density of the polymer and the polymer/solvent interactions, besides the ingredients added.

The mass of toluene sorbed by the NR/chitin composites was traced as a function of time in the sorption kinetics studies. The samples with filler loading from 0 up to 20 wt % were immersed in toluene, and the toluene uptake was determined in each case. It was observed that all the samples swelled upon immersion in toluene. In Figure 5 the toluene uptake up to equilibrium swelling is plotted vs time (the samples used to follow the kinetics studies were obtained from prevulcanized latex prepared by the evaporation method). It can be seen that for all compositions the uptake is rapid in the initial zone ($t < 5$ h). After this the sorption rate decreases leading to a plateau, corresponding to equilibrium swelling. The equilibrium toluene uptake values of vulca-

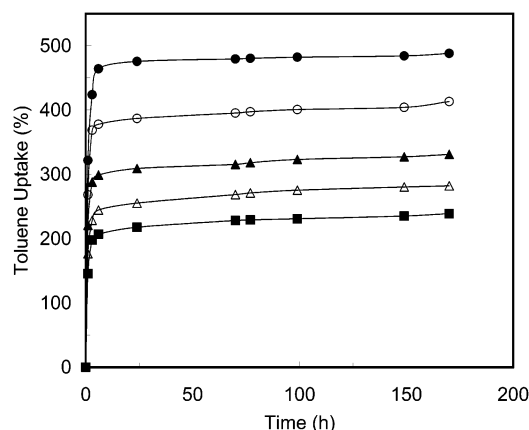


Figure 5. Variation in toluene uptake of PNRev (●), PCH5ev (○), PCH10ev (▲), PCH15ev (△), and PCH20ev (■) samples as a function of time at room temperature (25 °C). Solid lines serve to guide the eye.

Table 2. Toluene Uptake at Equilibrium and Toluene Diffusion Coefficients in Chitin Whiskers/Vulcanized NR Composites Immersed in Toluene

sample	toluene uptake at equilibrium (%)	toluene diffusion coefficient ($\text{cm}^2 \cdot \text{s}^{-1} \times 10^8$)
PNRev	488	14.1
PCH5ev	413	8.1
PCH10ev	331	5.0
PCH15ev	282	4.6
PCH20ev	239	4.4

nized NR/chitin composites are reported in Table 2. As the whisker content increases, it decreases continuously with a sharp evolution between 5 and 10 wt %.

The cross-link density of the evaporated matrix from prevulcanized latex was calculated from the classical equation,⁴⁰ and it was found to be around $13000 \text{ g} \cdot \text{mol}^{-1}$. The monomeric molecular weight of NR being $68 \text{ g} \cdot \text{mol}^{-1}$, the average number of monomer units between cross-links is of the order of 190.

In Figure 6, the weight swelling rate, $\phi_p = M_\infty/M_0$, is plotted for the samples prepared from the prevulcanized latex as a function of filler loading. For the unfilled matrix it was found to be around 5.9. For composite materials ϕ_p values were corrected to account for the fact that only the matrix phase can be swelled by the solvent. The filler weight must be removed from both M_0 and M_∞ data. As the whisker content increases, ϕ_p decreases. The corrected value is only around 4 for the 20 wt % chitin whisker filled composite. Therefore, the swelling of the material is strongly reduced in the presence of chitin whiskers within the NR matrix, and a decrease of around 50% is observed for the highly filled material (20 wt %). Similar results were reported for cellulose whisker filled plasticized starch when submitted to high moisture conditions.^{26,28} This phenomenon was ascribed to the formation of a rigid cellulose network, which prevented the swelling of the starch and therefore its water absorption. This three-dimensional network was found to result from the establishment of strong hydrogen bonding between cellulose whiskers that can develop during the film formation (evaporation step). Our finding most probably results from a similar phenomenon and can be ascribed, at least partially,

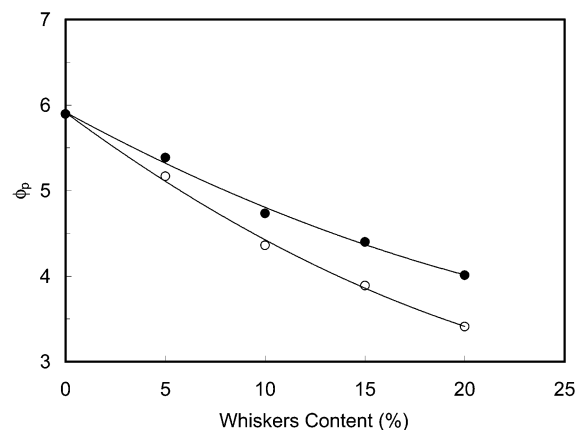


Figure 6. Raw (○) and corrected (●) weight swelling rate (ϕ_p) of vulcanized samples in toluene at room temperature (25 °C) as a function of chitin whiskers content. Solid lines serve to guide the eye.

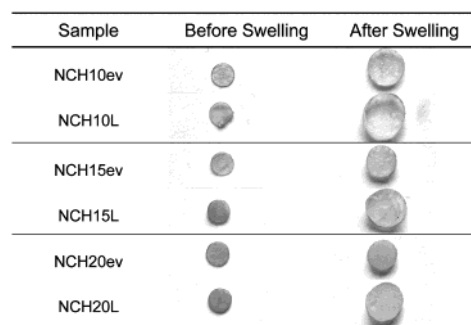


Figure 7. Photographs of unvulcanized samples (prepared by evaporation and hot-pressing methods) before and just after swelling in toluene for 24 h at room temperature (25 °C). The diameter of all samples before swelling was $d_0 = 7.5 \text{ mm}$.

to the formation of a chitin network within the vulcanized rubber. It can also result from strong interaction between the chitin filler and the cross-linked polymeric chains, preventing the swelling of the polymeric chains located in the interfacial zone.

The toluene diffusion coefficient, D , in the vulcanized NR-based composites was estimated as described in the Experimental Section. The D values are given in Table 2. The unfilled matrix presents the maximum diffusion coefficient (around $1.4 \times 10^{-7} \text{ cm}^2 \cdot \text{s}^{-1}$). Adding chitin whiskers within the NR matrix results in a progressive decrease of D value with a sharp evolution between 0 and 10 wt %, down to $4.4 \times 10^{-8} \text{ cm}^2 \cdot \text{s}^{-1}$ for the 20 wt % filled system. This observation could be attributed to the increasing stiffness of the hydrogen-bonded chitin network by increasing the filler content. It can also result from strong interaction between the filler and the matrix, which limits the toluene diffusivity within the entangled polymer matrix.

For unvulcanized samples, instead of following the above procedure, the bound rubber content and the fraction of NR dissolved in toluene were determined (details described in the Experimental Section) since part of the sample can dissolve in toluene during a long-term swelling experiment. Figure 7 shows photographs of unvulcanized NR/chitin whiskers nanocomposites before and 24 h after swelling in toluene. These photographs were recorded with a Nikon COOLPIX885 digital camera. It can be seen that all the samples swelled after immersion in toluene. It has also been

Table 3. Diameter (d) of Chitin Whiskers/Unvulcanized NR Composite Disks Immersed for 24 h in Toluene^a

sample	processing technique	d (mm)	diameter variation (%)
NCH10ev	water evaporation	12.5	67
NCH15ev		11	47
NCH20ev		10	33
NCH10L	freeze-drying and	15	100
NCH15L	hot-pressing	13.5	80
NCH20L		12.5	67

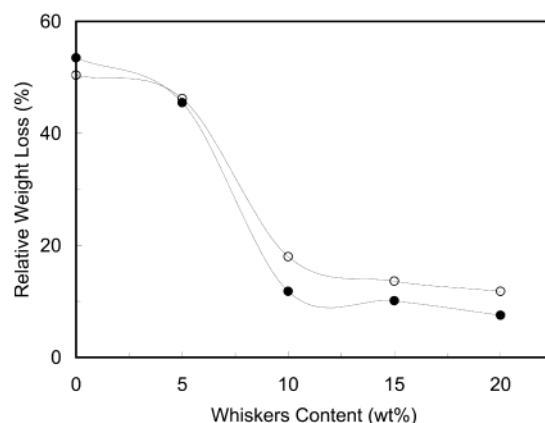
^a The initial sample diameter (before swelling) was $d_0 = 7.5$ mm and the diameter variation was determined by $(d - d_0)/d_0$.

observed that both pure unvulcanized NR and 5 wt % filled composite completely disrupted after 24 h of swelling; hence they are not included in Figure 7. By comparison of photographs of swelled evaporated samples (NCH10ev, NCH15ev, and NCH20ev), it clearly appears that swelling of the material systematically decreases with increasing amount of chitin whiskers within the NR matrix, as observed for vulcanized NR-based materials. This observation was quantified by measuring the diameter of the disk after 24 h of swelling in toluene. Results are reported in Table 3. For some compositions, swelling was not isotropic in the radial direction and the diameter was averaged. The diameter of the 10 wt % filled composite increased by 67% upon swelling. For the 20 wt % filled material the diameter increase was only 33%. As for vulcanized NR-based composites, this phenomenon can be explained, at least partially, by the formation of a hydrogen-bonded whisker network within the matrix. This stiff network hinders the swelling of the elastomer.

The effect of the processing technique on swelling can be analyzed by comparing evaporated and hot-pressed samples for a given composition (Figure 7 and Table 3). It is clearly observed that the degree of swelling upon toluene immersion is much higher for hot-pressed sample than evaporated sample at all compositions. It is also observed that the diameter of the swelled 10 wt % filled evaporated specimen (NCH10ev) is similar to that of 20 wt % filled hot-pressed (NCH20L) composite. A possible explanation could be ascribed to the fact that not only the presence of a chitin–chitin network but also the amount of whiskers affects the degree of swelling. From these results, it is assumed that the formation of a hydrogen-bonded network of whiskers within the matrix is a major reason for the lower degree of swelling exhibited by evaporated samples than hot-pressed samples. The evaporation method is a slow-step process, in which whiskers get enough time and mobility to establish a rigid chitin–chitin network within the host matrix. On the contrary, in the freeze-drying and subsequent hot-pressing method, the mobility of rubber chains and whiskers is completely arrested all on a sudden during initial quenching process. It results in the formation of filler aggregates within the matrix and which in turn causes poorer dispersion of chitin whiskers in the medium. SEM analysis (Figure 4e) supports this assumption. The very high elastic modulus of the evaporated composites compared to freeze-dried ones reported during the mechanical analysis (part 2) also revealed the presence of a chitin network in the former.

Table 4. Relative Weight Loss (RWL) and Fraction of Bound Matrix (FBM) of Chitin Whiskers/Unvulcanized NR Composite Disks Immersed for 48 h in Toluene and Dried for 12 h at 55–60 °C

sample	processing technique	RWL (%)	FBM (%)
NRev	water evaporation	53.5	0
NCH5ev		45.5	5.3
NCH10ev		11.8	36.6
NCH15ev		10.1	35.4
NCH20ev		7.5	35.3
NRL	freeze-drying and	50.4	0
NCH5L	hot-pressing	46.2	1.7
NCH10L		18.0	27.4
NCH15L		13.6	29.2
NCH20L		11.8	28.5

**Figure 8.** Relative weight loss of evaporated (●) and hot-pressed (○) unvulcanized samples after immersion in toluene at room temperature (25 °C) for 48 h and subsequent drying at 55–60 °C for 12 h. Solid lines serve to guide the eye.

The unvulcanized NR-based materials were also immersed in toluene for 48 h, dried for 12 h at 55–60 °C, and weighed as described in the Experimental Section. The bound rubber content and fraction of NR dissolved in toluene after 48 h were determined, and data are collected in Table 4. Figure 8 displays the evolution of the relative weight loss (RWL) versus chitin whiskers content for both evaporated and hot-pressed unvulcanized NR-based composites. Data show that about 50% of the unfilled material is dissolved in toluene. The dissolution of a limited amount of NR is ascribed to the fact that the experiment was performed at room temperature without any stirring. The RWL is slightly higher for the evaporated matrix (NRev) than for the hot-pressed one (NRL). It could be due to the formation of short cross-links developed in the NR during hot-pressing. As the whisker content increases, the RWL of the sample decreases with a sharp evolution between 5 and 10 wt %. For all composites, the RWL values are higher for hot-pressed samples than for evaporated ones. This observation can be ascribed again to the formation of a rigid chitin network within the evaporated materials. This network is expected to form above the critical volume fraction at the percolation threshold, v_{Rc} . For a 3D network, v_{Rc} depends on the aspect ratio L/d of the fiber as $v_{Rc} = 0.7/(L/d)$.⁴² For chitin whiskers obtained from crab shells, the aspect ratio close to 16 leads to a value of $v_{Rc} = 4.4$ vol %, i.e., around 6.4 wt %. This value is in the range

5–10 wt % for which the evolution of both the RWL and toluene uptake at equilibrium is fast. However, it seems that the influence of this network on the dissolution of NR chains is limited. The main parameter that is involved in this process is the presence of chitin whiskers and their level of interaction with the matrix. That is, the filler–matrix interactions should be sufficiently strong to prevent the dissolution of NR chains and maintain them in the “sol” fraction of the sample.

The fraction of bonded matrix (FBM) was determined from RWL data. It is worth noting that FBM values correspond to the NR fraction, which is entrapped within the network of chitin and on the surface of the chitin whiskers. For the calculation it was assumed that the insoluble part of the unfilled matrix ($1 - \text{RWL}_0$) should be present in the composites balanced by the matrix content ($1 - w_F$, w_F being the filler weight fraction). The “sol” fraction (% “sol”) of each sample is therefore the sum of three terms

$$\% \text{ “sol”} = 1 - \text{RWL} = w_F + (1 - \text{RWL}_0)(1 - w_F) + \text{FBM} \quad (1)$$

The first one (w_F) corresponds to the whiskers content, the second one $[(1 - \text{RWL}_0)(1 - w_F)]$ to the insoluble part of the matrix, and the third one (FBM) to the fraction of NR in strong interaction with the surface of the chitin filler. The FBM values calculated from eq 1 are collected in Table 4. It is interesting to see that FBM values first strongly increase with filler content and then stabilize for chitin whisker fractions higher than 5 wt %, i.e., above the percolation threshold. For low whisker content, it seems quite normal that the fraction of bonded matrix increases with the filler content as a result of the increase of the interfacial area. Above the percolation threshold, the interfacial area increases continuously but the following two phenomena can be appeared at high filler loading. On one hand, the overlapping of the whiskers restricts the filler/matrix interfacial area, and on the other hand, as the whisker network closes up, the entrapping matrix fraction decreases. These two effects are the responsible reasons for the stabilization of the FBM above the percolation threshold.

Conclusions

Chitin whisker reinforced natural rubber nanocomposites were developed from colloidal suspension of chitin whiskers and latex of both unvulcanized and prevulcanized natural rubber. The chitin whiskers, prepared by acid hydrolysis of chitin from crab shells, consisted of slender parallelepiped rods with an average length around 240 nm and an aspect ratio close to 16. After the aqueous suspensions of chitin whiskers and rubber were mixed and stirred, solid composite films were obtained by casting and evaporating methods. For unvulcanized systems a freeze-drying and subsequent hot-pressing processing technique was also used. All the results lead to the conclusion that the processing technique plays a major role in the properties of final composites developed. The nanosized chitin whiskers form a three-dimensional rigid network only in the evaporated samples, and it is assumed to be governed by a percolation mechanism. The critical volume fraction of chitin whiskers at the percolation

threshold was found to be 4.4 vol % (around 6.4 wt %). The morphology of samples was analyzed using SEM. The examination of the cryo-fractured surface of composite materials displays a better filler dispersion in the evaporated specimens than in the hot-pressed ones. It is ascribed to the fact that the evaporation method is a slow step process, in which whiskers get enough time and mobility to establish a rigid chitin–chitin network within the host matrix.

Swelling experiments using toluene provided additional insight regarding the existence of a chitin–chitin network in composite samples prepared by the evaporation method. The extent of swelling was different for evaporated and freeze-dried unvulcanized samples. The difference in the degree of swelling of various samples was determined by measuring the diameter of a circularly shaped sample, before and 24 h after swelling in toluene. It has been observed that unvulcanized evaporated samples are more resistant to swelling than freeze-dried ones because of the presence of a chitin network in the former. It has also been found that increasing the whisker content diminished the degree of swelling of samples in each method. The decrease in swelling of freeze-dried samples with increase in whisker content is attributed to the higher rigidity of the material as a result of the high amount of filler–matrix interaction. Both filler–matrix interaction and chitin network are the responsible reasons for the low degree of swelling with increase in whisker content exhibited by evaporated sample. The extent of filler matrix interaction in unvulcanized composite samples was determined by calculating RWL and the FBM after 48 h of immersion of samples in toluene and subsequent drying. For instance, the RWL and FBM values of 20 wt % whisker-filled evaporated samples are 7.5% and 35.3% and that of the corresponding freeze-dried samples are 11.8% and 28.5%, respectively, which indicates the presence of the three-dimensional chitin network in evaporated samples.

The decreasing tendency of diffusion coefficient values of vulcanized samples with increasing quantity of chitin whiskers is more evidence for the presence of chitin network in evaporated sample. The diffusion coefficient value of vulcanized NR was found to be $1.4 \times 10^{-7} \text{ cm}^2 \cdot \text{s}^{-1}$, and this value was successively reduced by the incorporation of whiskers. For example, for the 20 wt % filled composites the diffusion coefficient value is reduced to $4.4 \times 10^{-8} \text{ cm}^2 \cdot \text{s}^{-1}$.

Acknowledgment. The authors are grateful to Mrs. C. Crepeau (Technical Center, MAPA Company) and Safic Alcan for the supply of NR latex, Dr. M. Paillet for helping in chitin whiskers preparation, and Mrs I. Paintrand and D. Dupeyre for their help in TEM and SEM study, respectively. K. Gopalan Nair gratefully acknowledges the French Ministry of Research for its financial support.

References and Notes

- (1) Barlow, F. N. In *Rubber compounding principles and techniques*; Marcel Dekker: New York, 1993.
- (2) Blow, C. M.; Hepburn, C. In *Rubber Technology and Manufacture*, 2nd ed.; Butterworth-Heinemann: Oxford, 1982.
- (3) Liauw, C.M.; Allen, N. S.; Edge, M.; Lucchese, L. *Polym. Degrad. Stab.* **2001**, *74*, 159.

- (4) De, S. K.; White, J. R. In *Short fibre-polymer composites*; Woodhead Publishing: Cambridge, 1996.
- (5) Bounstany, K.; Hamed, P. *Rubber World* **1974**, 171, 39.
- (6) Beatty, J. R.; Hamed, P. *Elastomerics* **1978**, 110, 27.
- (7) Rogers J. W. *Rubber World* **1981**, 183, 27.
- (8) Ismail, H.; Shuhelmy, S.; Edyham, M. R. *Eur. Polym. J.* **2002**, 38, 39.
- (9) Ismail, H.; Edyham, M. R.; Wirjosentono, B. *Polym. Test.* **2002**, 21, 139.
- (10) Geethamma, V. G.; Thomas Mathew, K.; Lakshminarayanan, R.; Thomas, S. *Polymer* **1998**, 39, 1483.
- (11) Ismail, H.; Rozman, H. D.; Jaffri, R. M.; Mohd Ishak, Z. A. *Eur. Polym. J.* **1997**, 33, 1627.
- (12) Ismail, H.; Jaffri, R. M.; Rozman, H. D. *Polym. Int.* **2000**, 49, 618.
- (13) Ismail, H.; Jaffri, R. M. *Polym. Test.* **1999**, 18, 381.
- (14) Singh, D. K.; Ray, A. R. *J. M. S. Rev. Macromol. Chem. Phys.* **2000**, C40 (1), 69.
- (15) Rathke, D. R.; Hudson, S. M. *J. M. S. Rev. Macromol. Chem. Phys.* **1994**, C34 (3), 375.
- (16) Revol, J.-F.; Marchessault, R. H. *Int. J. Biol. Macromol.* **1993**, 15, 329.
- (17) Muzzarelli, R. A. A. Chitin microfibrils. In *Chitin*; Pergamon Press: New York, 1977; pp 51–55.
- (18) Brine, C. J.; Austin, P. R. Renatured chitin fibrils, films and filaments. In *Marine Chemistry in the Coastal Environment*; Church, T. D., Ed.; ACS Symposium Series 18; American Chemical Society: Washington, DC, 1975; pp 505–518.
- (19) Favier, V.; Canova, G. R.; Cavaillé, J. Y.; Chanzy, H.; Dufresne, A.; Gauthier, C. *Polym. Adv. Technol.* **1995**, 6, 351.
- (20) Helbert, W.; Cavaillé, J. Y.; Dufresne, A. *Polym. Compos.* **1996**, 17, 4, 604.
- (21) Dufresne, A.; Cavaillé, J. Y.; Helbert, W. *Polym. Compos.* **1997**, 18, 2, 198.
- (22) Dufresne, A.; Cavaillé, J. Y.; Helbert, W. *Macromolecules* **1996**, 29, 7624.
- (23) Dufresne, A.; Cavaillé, J. Y. *J. Polym. Sci., Part B: Polym. Phys.* **1998**, 36, 2211.
- (24) Dubief, D.; Samain, E.; Dufresne, A. *Macromolecules* **1999**, 32, 5765.
- (25) Dufresne, A.; Kellerhals, M. B.; Witholt, B. *Macromolecules* **1999**, 32, 7396.
- (26) Anglès, N. M.; Dufresne, A. *Macromolecules* **2000**, 33, 8344.
- (27) Anglès, N. M.; Dufresne, A. *Macromolecules* **2001**, 34, 2921.
- (28) Mathew, A. P.; Dufresne, A. *Biomacromolecules* **2002**, 3, 609.
- (29) Marchessault, R. H.; Morehead, F. F.; Walter, N. M. *Nature* **1959**, 184, 632.
- (30) Revol, J. F.; Marchessault, R. H. *Int. J. Biol. Macromol.* **1993**, 15, 329.
- (31) Li, J.; Revol, J. F.; Naranjo, E.; Marchessault, R. H. *Int. J. Biol. Macromol.* **1996**, 18, 177.
- (32) Revol, J. F.; Marchessault, R. H. *J. Colloid Interface Sci.* **1996**, 183, 365.
- (33) Paillet, M.; Dufresne, A. *Macromolecules* **2001**, 34, 6527.
- (34) Morin, A.; Dufresne, A. *Macromolecules* **2002**, 35, 2190.
- (35) Blackwell, J. *Methods Enzymol.* **1988**, 161 (Part B), 435.
- (36) Gaill, F.; Persson, J.; Sugiyama, J.; Vuong, R.; Chanzy, H. *J. Struct. Biol.* **1992**, 109, 116.
- (37) Hauser, E. A.; Le Beau, D. S.; Kao, J. V. L. *J. Phys. Chem.* **1942**, 46, 1099.
- (38) Gorton, A. D. T. Prevalcanised natural rubber latex for dipping. In *Proceedings of the International Rubber Technology Conference*, 1988; pp 85–103.
- (39) De Gennes, P. G. In *Scaling concepts in polymer physics*; Cornell University Press: London, 1979.
- (40) Treloar, L. R. G. In *The physics of rubber elasticity*; Oxford University Press: Oxford, 1975.
- (41) Flory, P. J. In *Principles of polymer chemistry*; Cornell University Press: London, 1953.
- (42) Favier, V. Ph.D. Thesis, Grenoble, France, 1995.

BM020127B